

Applications of transrectal ultrasound in prostate cancer

¹C J HARVEY, MRCP, FRCR, ²J PILCHER, MRCP, FRCR, ³J RICHENBERG, MRCP, FRCR, ²U PATEL, MRCP, FRCR and ⁴F FRAUSCHER, MD

¹Department of Imaging, Imperial Healthcare Trust, Hammersmith Hospital, London, UK, ²Department of Imaging, St George's Hospital, London, UK, ³Department of Imaging, Royal Sussex County Hospital, Brighton, UK, and ⁴Department of Radiology, Medical University Innsbruck, Innsbruck, Austria

ABSTRACT. Transrectal ultrasound (TRUS) was first developed in the 1970s. TRUS-guided biopsy, under local anaesthetic and prophylactic antibiotics, is now the most widely accepted method to diagnose prostate cancer. However, the sensitivity and specificity of greyscale TRUS in the detection of prostate cancer is low. Prostate cancer most commonly appears as a hypoechoic focal lesion in the peripheral zone on TRUS but the appearances are variable with considerable overlap with benign lesions. Because of the low accuracy of greyscale TRUS, TRUS-guided biopsies have become established in the acquisition of systematic biopsies from standard locations. The number of systematic biopsies has increased over the years, with 10–12 cores currently accepted as the minimum standard. This article describes the technique of TRUS and biopsy and its complications. Novel modalities including contrast-enhanced modes and elastography as well as fusion techniques for increasing the sensitivity of TRUS-guided prostate-targeted biopsies are discussed along with their role in the diagnosis and management of prostate cancer.

Received 23 May 2012
Accepted 28 May 2012

DOI: 10.1259/bjr/56357549

© 2012 The British Institute of
Radiology

Over 35 000 new cases of prostate cancer are diagnosed per annum in the UK and there are over 10 000 deaths annually [1–4]. It is the most common cancer in males in the UK, and causes 13% of all cancer deaths in males. The lifetime risk of being diagnosed with prostate cancer is one in nine. It has been estimated from post-mortem data that approximately half of all males in their fifties have prostate cancer, which increases to 80% by the age of 80 years, but only 1 in 26 men will die from their disease—supporting the fact that males are more likely to die with prostate cancer than from it [5, 6].

Over the last 20–30 years the incidence of prostate cancer has quadrupled, largely because of the introduction of widespread prostatic-specific antigen (PSA) testing, although the incidence in the UK may now have reached a plateau (UK Prostate Cancer Statistics, 2008 [7]). In the USA, the incidence peaked in 1992, and death rates have been decreasing since 1998 [8]. In the UK there has been a significant decline in the age-standardised mortality rate between 1993 and 2005, but the overall mortality rates have remained largely unchanged, as the decreasing mortality rate is counteracted by the aging population.

Risk factors for prostate cancer include age, a positive family history, abnormal digital rectal examination (DRE), raised PSA level and ethnicity. Black African and Caribbean men have two to three times the risk of being diagnosed with and dying of prostate cancer than white men, whereas Asian men have the lowest risk.

Prostate cancer can be divided into low-, intermediate- and high-risk disease, depending on the aggressiveness of the tumour. Since the 1970s there has been a marked change in the presentation of prostate cancer. Before PSA testing and transrectal ultrasound (TRUS) became widely available, most patients presented with cancer-specific symptoms owing to locally advanced disease and the cancers were diagnosed by DRE, so that the majority were diagnosed at stage T2 (Table 1) or more. Nowadays, most cases (>90%) are diagnosed at an asymptomatic early stage (stage T1) because the advent of widespread PSA testing and TRUS-guided biopsy has enabled early diagnosis, with nearly half of all newly diagnosed patients falling into the “favourable risk” group. Over the past 20 years the proportion of males with low- vs high-risk disease at diagnosis has shifted significantly from 29.5% vs 36.6% (1989–1992) to 46.8% vs 16.0% (2000–2002) [9]. Liberal screening with PSA testing (Table 2), however, does have its disadvantages, with a significant false-positive rate (only 30% of males with an elevated PSA level will have cancer) and a recognised false-negative rate (15% of men with PSA < 4 ng ml⁻¹ will have a cancer focus). It is also unable to distinguish between aggressive and indolent cancers.

Currently there is no formal national screening policy for prostate cancer, although opportunistic screening in primary care does occur in males presenting with lower urinary tract symptoms.

Two recent reviews of several randomised controlled trials concluded that there was insufficient evidence to support the use of PSA testing to screen for prostate cancer and its use may potentially cause harm [10, 11]. Screening for prostate cancer does not have a significant impact on either overall mortality or death from prostate cancer.

Address correspondence to: Dr Chris Harvey, Department of Imaging, Imperial Healthcare Trust, Hammersmith Hospital, Du Cane Road, London W12 0HS, UK. E-mail: chris.harvey@imperial.nhs.uk

Table 1. Tumour–node–metastasis (TNM) staging for prostate cancer

T	Tumour
T0	No evidence of primary tumour
T1	Tumour neither palpable on DRE nor seen on imaging
T1a	Positive incidental histological finding in <5% of the tissue resected
T1b	Positive incidental histological finding in >5% of tissue resected
T1c	Cancer identified on biopsy performed because of elevated PSA level
T2	Tumour palpable on DRE and confined to the gland
T2a	Tumour involves <0.5 of one lobe
T2b	Tumour involves >0.5 of one lobe but not both lobes
T2c	Tumour involves both lobes
T3	Tumour extends through prostatic capsule and/or involves the seminal vesicles
T3a	Extracapsular extension (unilateral or bilateral) including microscopic bladder neck involvement
T3b	Tumour invades seminal vesicle(s)
T4	Tumour is fixed or invades adjacent structures other than seminal vesicle: external sphincter, rectum, levator muscles and/or pelvic wall
N	Regional lymph nodes
NX	Regional lymph nodes cannot be assessed
N0	No regional lymph node metastasis
N1	Regional lymph node metastasis
M	Distant metastasis
MX	Distant metastasis cannot be assessed
M0	No metastasis
M1	Distant metastasis
M1a	Metastases to non-regional lymph nodes (outside of the pelvis)
M1b	Metastases to bones
M1c	Metastases to other distant organs such as lungs, liver or brain

DRE, digital rectal examination; PSA, prostatic specific antigen.

Screening helps to diagnose prostate cancer at an earlier stage but the benefit-to-risk ratio remains uncertain because of significant morbidity associated with treatment.

Transrectal ultrasound

Normal appearances

TRUS was pioneered in the early 1980s [12]. Modern transducers typically are end-firing probes scanning at frequencies of 5–10 MHz. The prostate is divided into distinct anatomical zones (Figure 1) and these can be depicted by TRUS [13, 14] (Figure 2). The peripheral zone

(PZ) is echogenic relative to the central zone (CZ) and the transition zone (TZ), which are echopoor. The CZ is difficult to distinguish from the TZ in a healthy adult. In young males the PZ constitutes 75% of the gland volume, the CZ 20% and the TZ 5%, but these ratios will change with age and the onset of benign prostatic hypertrophy (BPH). BPH starts in the TZ and can eventually occupy most of the gland, stretching and thinning the PZ. Within the central gland, the ejaculatory ducts can be visualised as echogenic tramlines on longitudinal scans. These can be traced posteriorly to the ampulla of vas, where the seminal vesicles join. Between the seminal vesicles the vas deferens can be seen arising from the ampulla of vas. The bladder neck (fuses with the prostate) and external urethral sphincter (distal to the prostatic apex) can be seen as slightly echopoor structures (owing to anisotropy from orientation of smooth muscle fibres) relative to the prostate. The prostate does not have a true capsule, but a clear boundary can be seen around the prostate–fat interface and this has been termed the prostatic capsule. It is normally smooth and regular. The neurovascular bundles can be identified posterolateral to the prostate in the fat-filled echogenic triangular-shaped space between the seminal vesicles and the prostate. This is of relevance to the sonologist as this is the site where local anaesthesia may be introduced and also is a site of potential capsular weakness prone to local tumour spread. The levator ani muscles are seen as linear structures lateral to the prostatic bed.

The gland volume is calculated using an ellipsoid formula by measuring the maximum anteroposterior, craniocaudal and transverse distances and multiplying the product of these by $\pi/6$ (Figure 3). Inspection of the gland should focus on identifying asymmetry, areas of increased vascularity, hypoechogenicity and the presence

Table 2. Prostatic specific antigen (PSA)

Age (years)	Normal range of PSA (ng ml ⁻¹)
40–49	0.0–2.5
50–59	0.0–3.5
60–69	0.0–4.5
70–79	0.0–6.5

PSA is a kallikrein-like serine protease secreted by epithelial cells in the prostate gland and measured in the blood.

Serum levels rise when there is disruption of the basal layer/basement membrane due to infection, inflammation, malignancy or after prostate manipulation. Therefore, PSA is organ- but not cancer-specific.

An age-specific normal level can be defined.

Levels outside this range denote a raised risk of cancer, the risk rising with the level of PSA. PSA <10 ng ml⁻¹ has a positive predictive value (PPV) of 25%, whereas PSA >10 ng ml⁻¹ has a PPV of 58% for prostate cancer.

A cut-off of 4 ng ml⁻¹ confers a sensitivity of 67.5–80.0% in screening for prostate cancer.

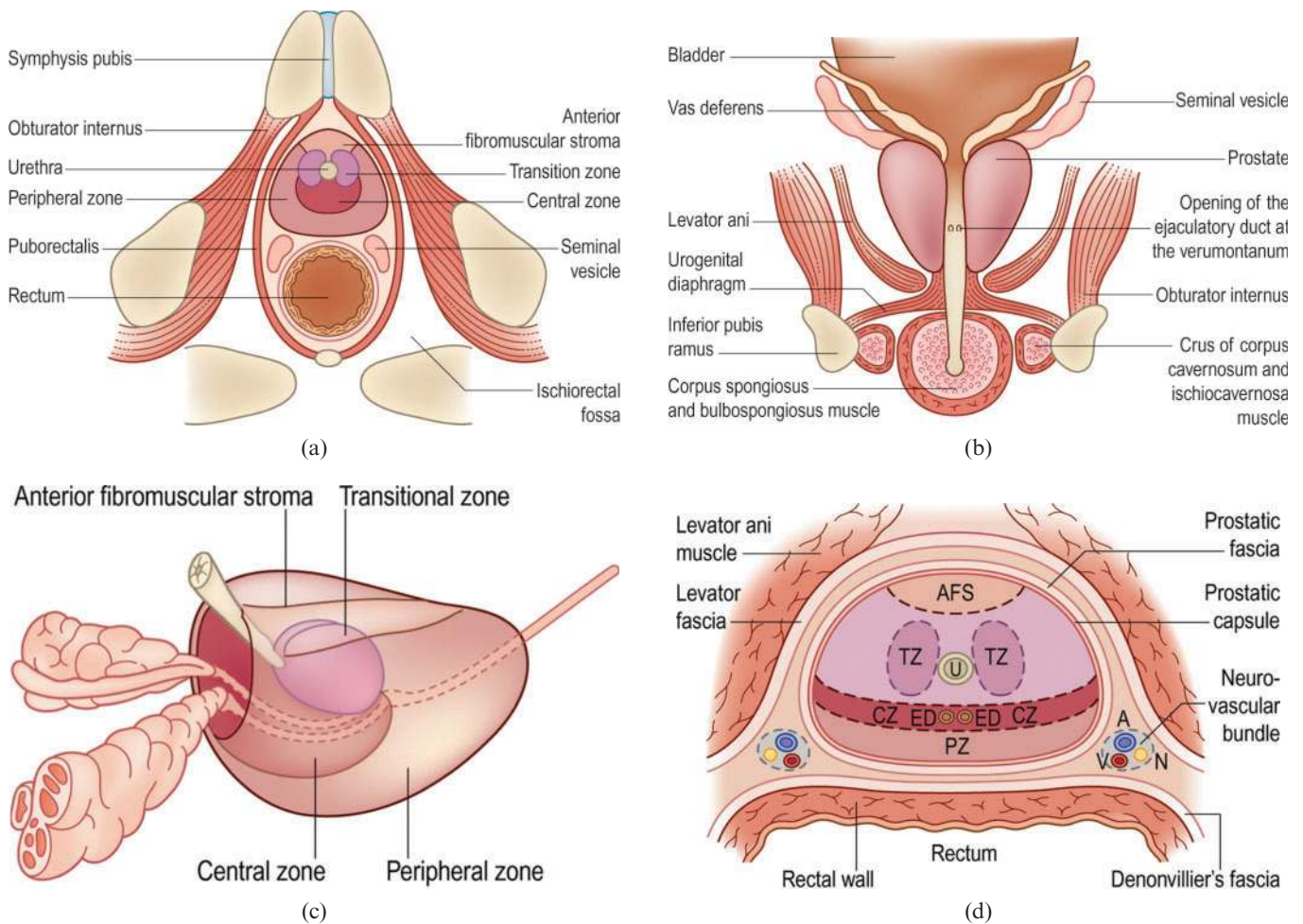


Figure 1. Anatomy of the prostate gland and surrounding structures. (a, b) Axial and coronal views of the prostate gland and its close anatomical relationships. (c) Zonal model of the prostate. (d) Fascial planes around the prostate. A, artery; AFS, anterior fibromuscular stroma; CZ, central zone; ED, ejaculatory duct; N, nerve; PZ, peripheral zone; TZ, transition zone; U, urethra; V, vein. Reproduced with permission from [14].

of focal bulges, irregularity or breaches of the capsule. These features are associated with the presence of cancer and should be documented, but are not sufficiently reliable to make a diagnosis without obtaining a biopsy.

Transrectal ultrasound biopsy

Current indications for prostate biopsy are given in Table 3. Absolute contraindications to TRUS biopsy include surgical absence of rectum, ilio-anal pouch, inflammatory bowel disease (especially Crohn's disease) and severe bleeding diatheses. It is recommended that patients on anticoagulation should have their international normalised ratio (INR) corrected to ≤ 1.3 . Relative contraindications to biopsy are acute prostatitis, perianal inflammation and severe haemorrhoids. Written consent should be obtained. The patient's bladder should ideally be empty before the procedure. Prophylactic antibiotics should be administered according to local protocol (see below).

The patient is then positioned in the left lateral decubitus or lithotomy position, an endorectal probe with the biopsy guide is inserted and local anaesthetic administered around the prostate.

Anaesthesia

The application of local anaesthetic is now standard practice [15–17]. 10 ml of 1% lidocaine is administered via a long 22-G Chiba needle (Cook Medical, Bloomington, IN) [18]. The anaesthetic may be administered around the neurovascular bundle between the base of the gland and the seminal vesicles (Figure 4), adjacent to the apex or into Denonvilliers' fascia. None of the sites has been shown to be superior but it is the authors' practice to inject 2.5 ml at the base and apex bilaterally. It should be noted that injecting directly into the gland is of no benefit. Potential complications of local anaesthesia use include pain caused by needle puncture, systematic lidocaine toxicity, temporary urinary incontinence (because of anaesthesia of the external urethral sphincter), artefact formation on the TRUS image (from air introduced during injection), periprostatic infection and erectile dysfunction [19]. The incidence of all these is very low and other studies have found no significant complication rates with the use of local anaesthesia [20, 21].

Antibiotic prophylaxis

Antibiotic prophylaxis is standard because of the potential for infection, with *Escherichia coli*, anaerobes and

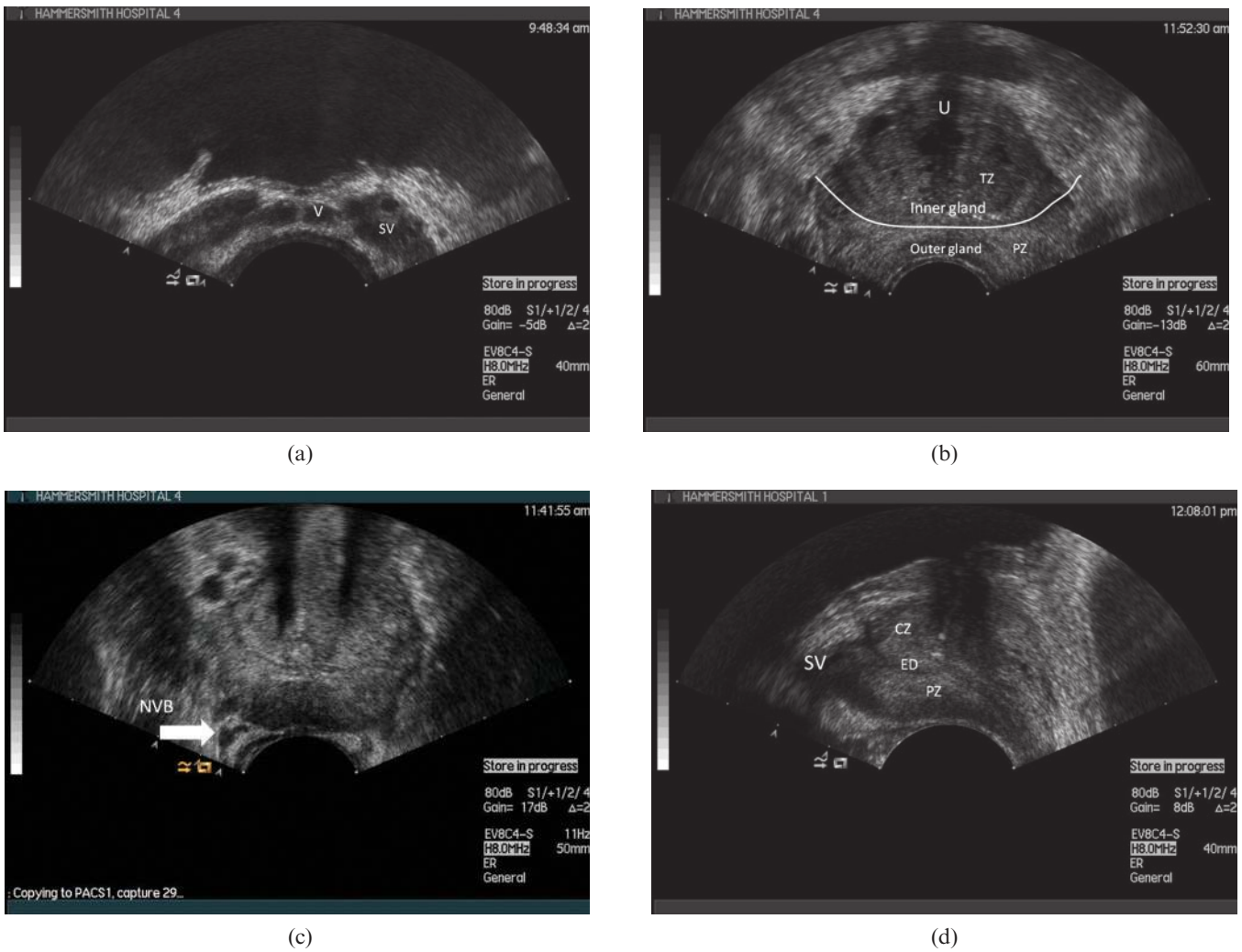


Figure 2. Axial transrectal ultrasound (a–c) and longitudinal images of the normal prostate (d). CZ, central zone; ED, ejaculatory duct; NVB, neurovascular bundle; PZ, peripheral zone; SV, seminal vesicle; TZ transition zone; U, urethra; V, vas deferens.

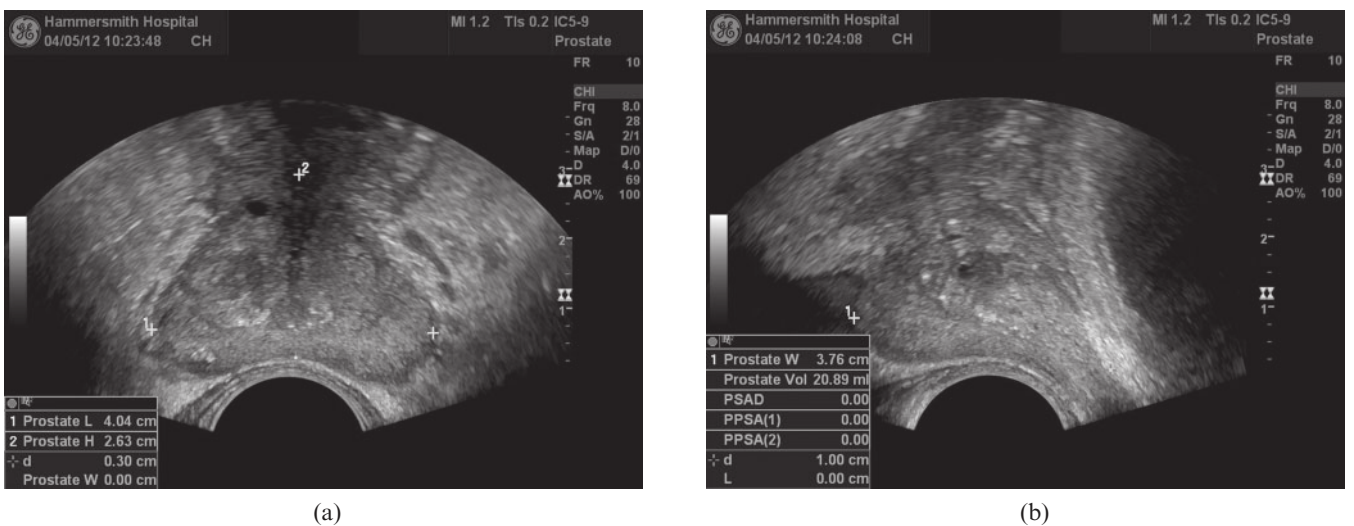


Figure 3. Method of measurement of prostatic volume on axial (a) and sagittal planes (b).

Table 3. Current indications for prostate biopsy

Elevated total PSA
Free PSA <20%
PSA velocity >0.75 ng ml ⁻¹ per year
Abnormal digital rectal examination
Previous negative biopsies, but continuing high suspicion for prostate cancer

PSA, prostatic specific antigen.

Gram-positive organisms being the most commonly identified [22].

Post-biopsy infection rates without antibiotic prophylaxis are quoted as 1–6%, resulting in septicaemia requiring hospitalisation in 0–4% (pooled data) [23].

Lee et al [24] found that the quinolones (predominantly ciprofloxacin) are the most commonly used prophylactic antibiotics. Current guidelines recommend a minimum of one oral antibiotic, such as a quinolone [25]. This is best commenced a few hours before the biopsy on the day of the procedure and may be continued for 3–5 days afterwards [26]. Shorter courses of quinolones, with intravenous gentamicin at the time of the biopsy, may also be used. Additional prophylaxis is required in patients at risk of endocarditis. Worryingly, a rise in antibiotic-resistant organisms has been recently reported in patients after TRUS biopsy [27]; therefore, infection rates and local patterns of resistance should be regularly audited.

Complications and side-effects

The overall complication rate of TRUS-guided prostate biopsy remains low. The risks of infection and rectal bleeding are 0–4% and 1.3–5.8%, respectively, in pooled data [23, 27, 28].

Complications of TRUS-guided biopsy are shown in Table 4, with the range of reported incidences. Increasing the number of biopsies has been associated with an

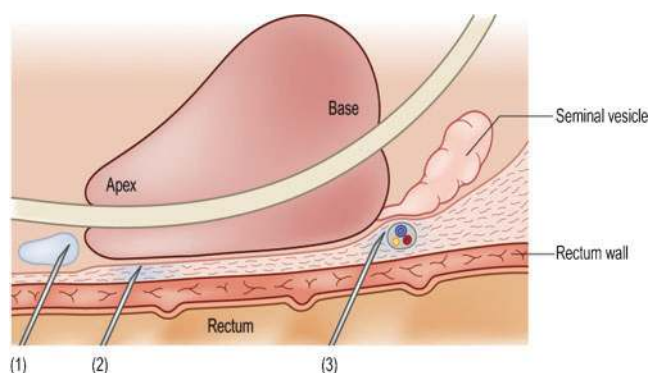


Figure 4. The various methods for anaesthetising the prostate gland. In (1) the needle is positioned just outside the apex and the local anaesthetic is injected to create a pool around it. In (2) the injection has been made into Denonvilliers' fascia, just beyond the rectal wall. In (3) the local anaesthetic has been introduced around the neurovascular bundle, between the base of the gland and the seminal vesicle. Any of these sites can be used, as none is of proven superiority, but both sides should be injected for maximal effect. Reproduced with permission from [14].

increase in urinary retention and epididymitis. Urinary retention is thought to be due to prostatic oedema and may occur in the absence of haematuria.

Haemorrhage

The incidence of haemorrhage increases with the number of biopsies. Severe haemorrhage requiring hospitalisation is rare: it is almost always per rectum from a rectal vein or artery, and may occur some hours after biopsy. Hospitalisation and transfusion are often necessary, and urgent proctoscopy to cauterise any bleeding points is indicated for suspected arterial bleeds. Direct compression of the rectal mucosa with the TRUS probe or a rectal balloon may help as a temporary measure.

Aspirin and non-steroidal anti-inflammatory drugs have not been conclusively shown to increase the frequency or severity of haemorrhagic complications [29]. Warfarin should be stopped until the INR is <1.3. Similarly, clopidogrel must also be stopped for 7 days prior to biopsy. Anticoagulants are restarted 24 h after biopsy. If anticoagulation/antiplatelet agents cannot be safely discontinued, the patient should be converted to heparin and biopsied as an inpatient. Haematuria is the commonest form of haemorrhage, but haemospermia can last longest.

Biopsy number and technique

18G (Tru-Cut) core biopsy needles (Tru-Core Angiotech, Gainesville, FL) are currently accepted as standard for the histological diagnosis of prostate cancer. The number of biopsies has increased since the original sextant biopsy developed by Hodge et al [30]. 10 or 12 cores are now the standard in the UK and Europe, carried out in a systematic way according to number (Figure 5) [25, 31]. The increasing number of biopsies reflects the isoechoic nature of the occult, small, multifocal cancers commonly encountered in modern practice. Thus, sampling is systematic and not random with the biopsies sampling the PZ, as this is the most likely site of cancer. However, there is still wide variation in the number of cores taken, direction of needle and area targeted. This is reflected in large variations in cancer detection between centres and also in the fact that increasing the number of cores will increase both cancer detection and complication rates [32]. In the ProtecT study [28] cancer detection rates varied from 23% [95% confidence interval (CI) 14–36%] to 53% (CI 40–65%) across eight centres. It should also be noted that the current systematic biopsy protocols do not sample the inner gland because of its lower cancer rate and lower metastatic potential. Eichler et al [33] analysed 87 studies (20 698 patients) and concluded that schemes of 12 cores that included posterior/laterally directed cores struck a balance between detection rate and adverse events.

Interpreting biopsy results

Prostate biopsy is used to confirm the clinical diagnosis of malignancy and stratify tumour aggressiveness. The Gleason grading system characterises the "aggressiveness" of prostate cancer and is central to the

Table 4. Complications associated with transrectal ultrasound biopsy

Complication	% of biopsies
Haematospermia	37.4
Bleeding from urethra, urinary bladder (>1 day)	14.5
Fever	0.8
Urosepsis	0.3
Rectal bleeding <2 days	2.2
Rectal bleeding >2 days requiring surgical intervention	2.2
Urine retention	0.2
Prostatitis	1.0
Epididymitis	0.7
Other complications requiring hospitalisation	0.3

Percentage given per biopsy session, irrespective of number of cores.

Adapted from National Comprehensive Cancer Network. Clinical practice guidelines in oncology. Prostate cancer early detection, v.2.2010. Fort Washington, PA: NCCN; 2010. p. 15. Available from: http://www.nccn.org/professionals/physician_gls/PDF/prostate.pdf

management and risk stratification of all prostate cancers. A five-point scale is used to categorise the cellular architecture within a biopsy core from very well differentiated to undifferentiated. Because of the multifocal nature of prostate cancer, and the heterogeneity of the cellular architecture, the Gleason score or sum is derived by adding together the two most common Gleason grades across the cores. The worst score should be incorporated into the score even if this constitutes <5% of the cancer. The combined score ranges from 2 to 10. A score of <4 is an indolent well-differentiated tumour; 5–7 is of intermediate risk; and a score of 8–10 places the tumour as clinically aggressive. Most cancers currently diagnosed are scored either 6 or 7. Within these scores the predominant grade of cell (the first number) is important, e.g. a Gleason grade of 4+3 is more aggressive than a grade of 3+4, although both are Gleason score 7.

In a proportion of men prostate biopsy is falsely negative: either the tumour is located in the central part of the gland or the cancer focus is small. A false-negative result may be suspected if an initial biopsy has shown numerous foci of high-grade prostate intra-epithelial neoplasia (HGPIN) (Table 5), if the PSA level continues

to rise or if the DRE remains suspicious. The appropriate treatment in these cases is repeat biopsy, usually taking more cores including biopsy of the central gland. In some cases, a saturation biopsy protocol is necessary.

However, HGPIN as an isolated finding is no longer considered an indication for repeat biopsy [25]. A repeat biopsy should therefore be prompted by other clinical features, such as DRE findings and PSA level. If HGPIN is extensive (*i.e.* multifocal biopsy sites), this is an indication for careful surveillance or early repeat biopsy because of the increased risk of prostate cancer.

Other surrogate indicators of tumour volume are the number of positive biopsies (especially if bilateral), the percentage of each core involved and the presence of perineural invasion or capsular breach.

Prostate cancer detection

TRUS remains the first modality of choice for imaging the prostate. Yet, despite technological advances in high-frequency wideband probes, greyscale ultrasound has an accuracy of only 50–60% with a positive predictive value

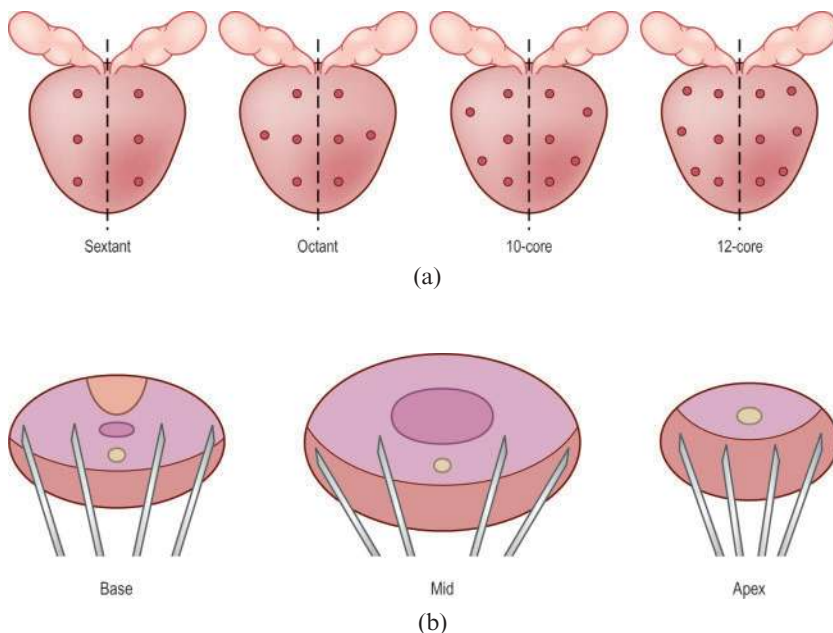


Figure 5. Principles behind prostate biopsy. (a) The various biopsy schemes used, in the coronal plane. The first is the classic sextant pattern, which misses about 25% of cancers. The next three schemes illustrate the octant, 10-core and 12-core regimes, respectively. In current practice the 10- or 12-core regime is favoured. (b) Prostate biopsy is a systematic sampling technique and the diagram shows that the cores are preferentially targeted onto the peripheral zone as most cancers occur here. Note how the trajectories are aimed anterolaterally to maximise peripheral zone sampling. Reproduced with permission from [14].

Table 5. Prostate intra-epithelial neoplasia

Excessive cellular proliferation is seen within ducts, ductules and acini, with an intact basal membrane. It can be graded as low or high grade (HGPIN), but only the latter is clinically relevant
 HGPIN is postulated to be a precursor to prostate cancer, with studies suggesting it pre-dates frank cancer by approximately 10 years. When found on biopsy the concern is that it may already be associated with cancer and 30–50% of patients with HGPIN will have concurrent cancer
 However, HGPIN as an isolated finding is no longer considered an indication for repeat biopsy [25]. A repeat biopsy should therefore be prompted by other clinical features, such as digital rectal examination findings and PSA level. If HGPIN is extensive (*i.e.* multifocal biopsy sites), this is an indication for careful surveillance or early repeat biopsy because of the increased risk of prostate cancer

HGPIN, high-grade prostate intra-epithelial neoplasia; PSA, prostatic specific antigen.

as low as 6% for the detection of prostate cancer. Its accuracy for local staging is also relatively poor.

Classically 70% of cancers originate from the PZ, 10% from the CZ and 20% from the TZ [34]. 60–70% of cancers are echopoor (Figure 6), but only 17–57% of echopoor foci are malignant. 30–40% of cancers are isoechoic and a small percentage are echogenic. Of sonographically visible cancers 30% appear as a focal nodule, whereas a focal lesion is accompanied by an infiltrative component in 50% and an infiltrative pattern predominates in approximately 20%.

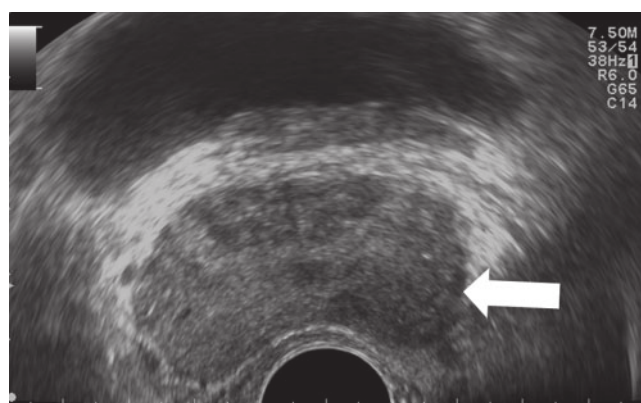
Studies employing targeted biopsies of focal lesions have given variable results. Gosselaar et al [35] studied 1840 males in whom 532 cancers were detected, but only 3.5% of visible cancers were detected solely by the additional biopsy.

Toi et al [36] reviewed 7426 biopsies and found that the presence of a sonographic lesion significantly increased the likelihood of cancer detection (50.7% *vs* 30.8%), with positive biopsies from lesions having a greater percentage of the core involved with cancer (50% *vs* 10%), and they were more likely to have Gleason score ≥ 7 (69.0% *vs* 28.3%).

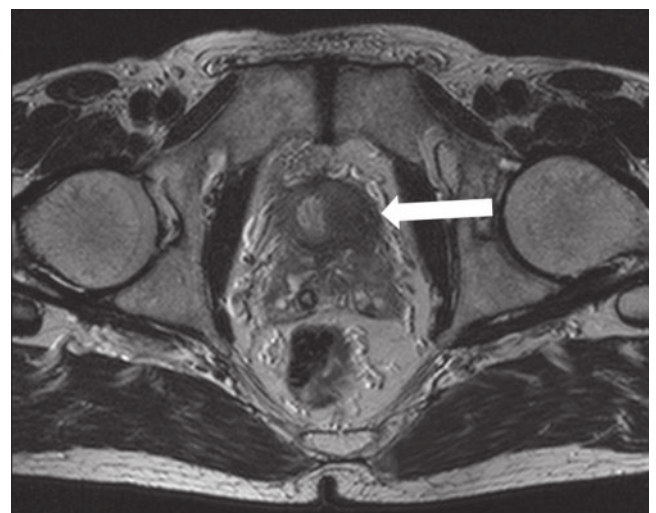
However, TRUS is limited in detecting prostate cancer because of the variability in ultrasound appearances, the poor specificity of sonographic abnormalities, the fact that tumours are frequently multifocal and the significant proportion of isoechoic cancers which cannot be

differentiated from benign changes [37]. In addition to this, the mixed echo pattern of BPH may mask any central gland tumour as it is indistinguishable from BPH [38]. Underdetection of anterior tumours is also a problem, especially in the setting of BPH.

The traditionally described echopoor lesion in the PZ has become a less frequent finding, with most contemporary prostate cancers tending to be either isoechoic or showing non-specific echo-irregularity, which may be the result of increased PSA testing and downward stage migration of prostate cancer at presentation. A correlation with PSA level and tumour sonovisibility has been noted [13]. If the PSA level is $>20 \text{ ng ml}^{-1}$, $>75\%$ of tumours are seen, whereas $<30\%$ are seen at a PSA level $<10 \text{ ng ml}^{-1}$ (the current situation in modern practice). Although the appearances of tumour are variable, the following are strongly suspicious of carcinoma: echopoor nodule in the PZ; diffuse echopoor change in the PZ; nodule with surrounding altered echogenicity; and a hypervascular echopoor nodule in the PZ [13, 34]. A capsular bulge associated with an echopoor or isoechoic nodule or an irregular capsule margin may also be signs of a cancer (Figure 7). However, these findings are not specific and hyperplasia, HGPIN, prostatitis (Figure 8) and necrosis can all have similar appearances. Recognised areas of increased incidence of cancer are the posterolateral horns, the prostate base close to the seminal vesicle and the apex, which are relative “blind”



(a)



(b)

Figure 6. A prostate cancer is seen as a focal echopoor lesion (arrow) with capsular invasion on axial transrectal ultrasound (a). T_2 weighted axial MRI (b) confirms stage T3a with capsular invasion sparing the left seminal vesicle (arrow).

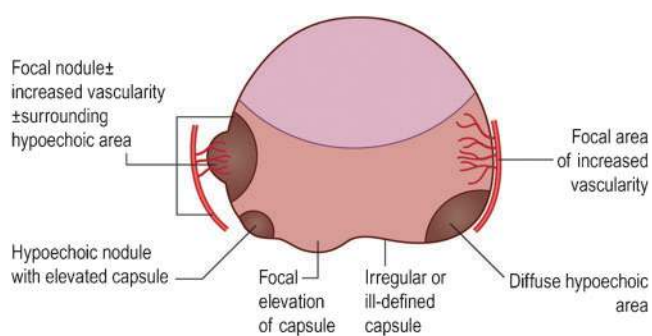


Figure 7. Transrectal ultrasound appearances suspicious for cancer. Reproduced with permission from [14].

areas (Figure 9) [14]. These areas should be carefully assessed in two planes comparing greyscale and vascularity with the contralateral side.

The accuracy of TRUS for local staging is poor, with sensitivity, specificity and accuracies of 50–92%, 46–91% and 58–86%, respectively, for extracapsular extension (T3 disease). TRUS signs of extracapsular extension are focal bulges, irregularity of the capsule and echopoor stranding of the periprostatic fat. For seminal vesicle involvement (Figure 10) the sensitivity, specificity and accuracies are 22–60%, 88% and 78%, respectively [14]. This compares badly with a sensitivity and specificity of MRI for staging of 91% and 96%, respectively.

Role of colour and power Doppler

The normal prostate gland has little flow, but what is present is usually symmetrical. However, strong Doppler signal may be seen in the neurovascular bundles and pericapsular and periurethral arteries. Initially, it was thought that the use of colour/power Doppler techniques increased the detection of cancer, but it transpired that it had a poor specificity with some cancers appearing

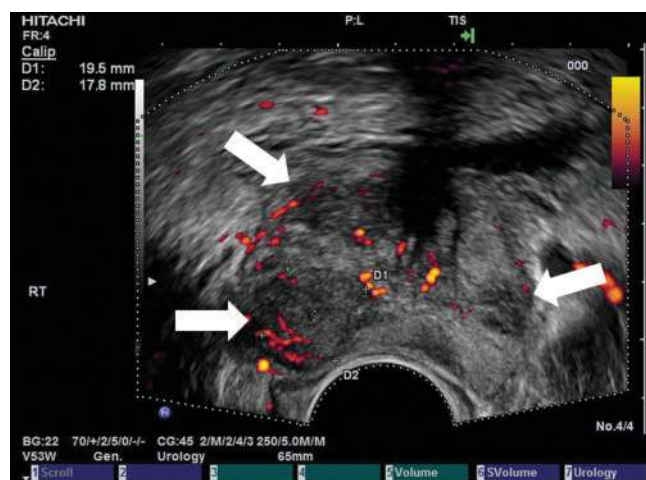


Figure 8. Prostatitis mimicking carcinoma. A 68-year-old male with an incidental raised prostatic specific antigen level but no urinary symptoms. Axial transrectal ultrasound shows multifocal echopoor lesions with increased vascularity (arrows) that were thought to represent carcinoma sonographically. Biopsy revealed multifocal acute inflammation with no malignancy.

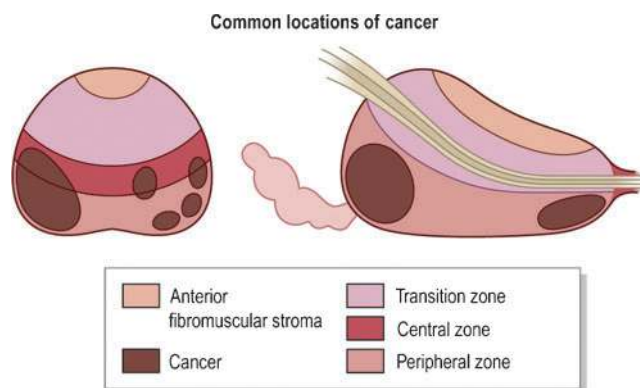


Figure 9. Common locations of prostate cancer. Reproduced with permission from [14].

hypovascular and some benign lesions showing increased vascularity [39]. Although more sensitive than colour Doppler, power Doppler has not been shown to be significantly better [40]. Turgut et al [41] found that spectral waveform analysis of the capsular and urethral arteries of the prostate using power Doppler may be useful in differentiating cancer from benign hypertrophy. Three patterns of flow changes have been noted in cancer: focal flow (Figure 11), increased flow around a nodule and asymmetrical flow on the cancerous side with an increase in the size and number of vessels. Overall, the use of conventional Doppler increases the specificity by about 5–10% [42]. Thus, conventional Doppler techniques are not specific and sensitive enough to replace the systematic biopsy protocol. However, targeted biopsies of focal vascular areas, when present, should be performed in addition to systematic sampling and especially in those undergoing repeat biopsy.

Ultrasound microbubbles

Angiogenesis is known to be essential for tumour growth and invasion. Pathological analysis of prostate tumours demonstrates increased microvessel density compared with the surrounding normal parenchyma [43].

Imaging techniques that allow quantification of blood flow in these microvessels may provide the opportunity to significantly improve prostate cancer detection and characterisation [44, 45]. Despite changes in biopsy practice and technological advances which have improved detection rates, there are still significant false-negative rates that have prompted the evaluation of microbubble contrast agents (Figure 12). The aspiration is to use targeted biopsy instead of the systematic multicore approach, so reducing the potential adverse effects of multiple biopsies, and to diagnose aggressive tumours that are clinically important and exclude indolent cancers.

Tumour vessels are of the order of 10–50 µm in diameter, which is well below the 1-mm resolution limit of conventional Doppler techniques. Microbubble-specific techniques allow imaging of vessels down to 50–100 µm in diameter [46, 47]. In addition, since microbubbles are vascular tracers, by following the passage of a bolus injection through a tissue of interest, time–intensity

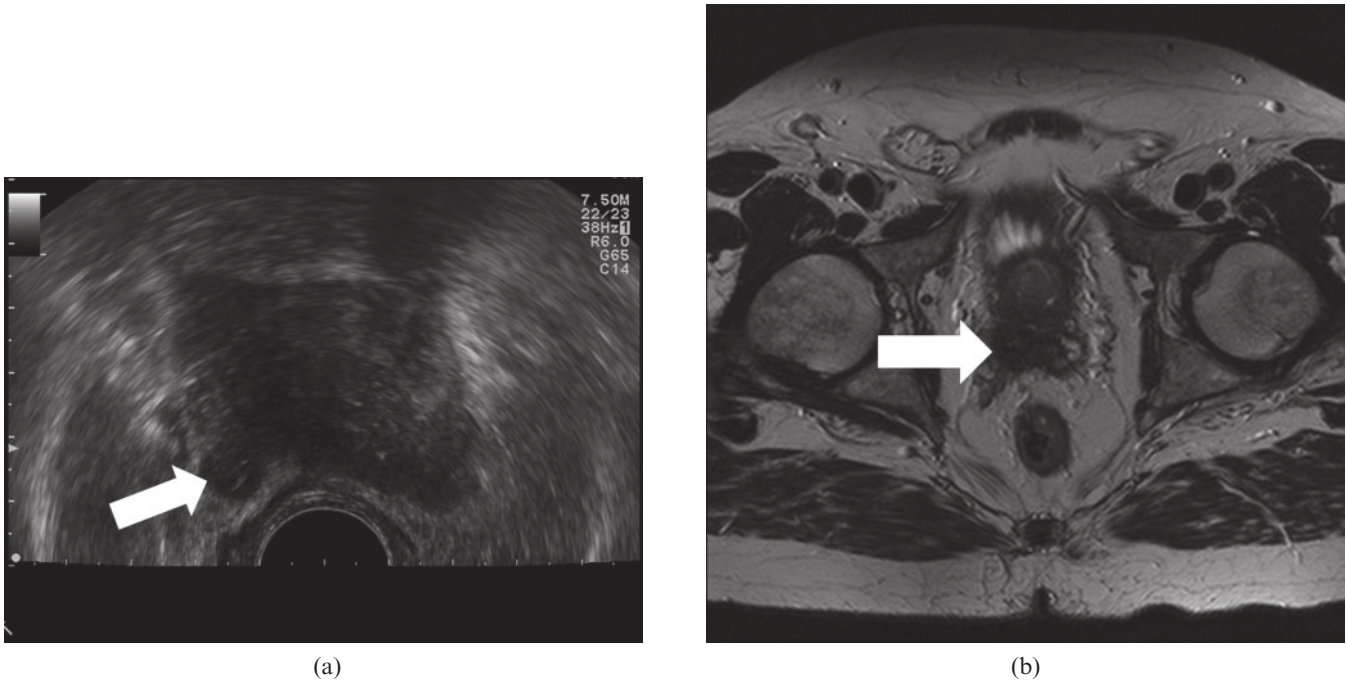


Figure 10. Stage T3b right Gleason 4+4 cancer on axial transrectal ultrasound (a) showing seminal vesicle invasion (arrow), confirmed on axial T_2 MRI (b).

curves may be generated (Figure 13) from which many functional indices [47–50] can be derived, including bolus arrival time, time to peak intensity, area under the curve and washin/washout curves as well as more complex indices. The indices derived can be used to construct true functional images by displaying them on a pixel-by-pixel basis as an overlay on the greyscale image (Figure 14) [49]. Grossen et al [50] showed that the time to peak enhancement was the most predictive parameter for the localisation of the malignant lobe of the prostate, with 78% of patients correctly diagnosed. Quantitative methods can be employed based on the destruction of microbubbles and observing the effects on contrast enhancement (reperfusion kinetics). Intermittent

high-power ultrasound pulses may be used to destroy microbubbles within a beam, and the rate of replenishment in the field can be used to calculate microbubble flow rate, a surrogate of perfusion and fractional vascular volume [51].

Halpern et al [52], using contrast-enhanced real-time and intermittent harmonic imaging in addition to power Doppler, showed a significant increase in sensitivity from 38% to 65% while specificity was maintained at 80% in cancer detection. These results have also been found by other workers [53]. Using Levovist[®] contrast agent (Schering AG, Berlin, Germany) and a colour Doppler-based targeted biopsy protocol, Frauscher et al [54] showed that positive biopsy rates were significantly

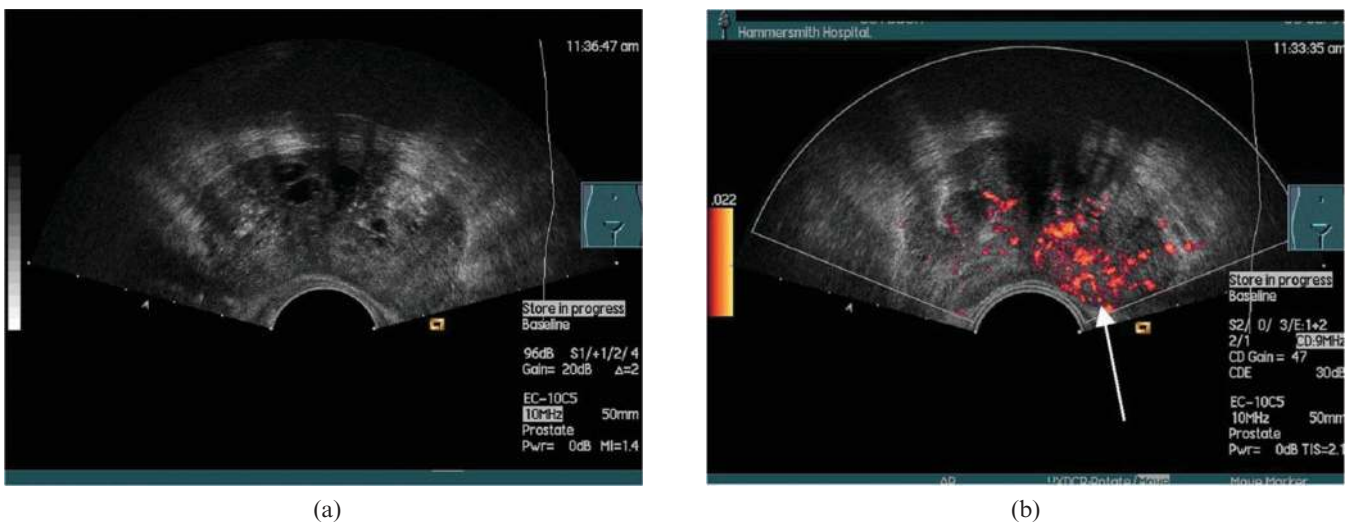


Figure 11. Prostate cancer. (a) Greyscale transverse ultrasound section of a prostate with no focal abnormalities visible. (b) Power Doppler (unenhanced) of the same section shows a focal hypervascular area (arrow) demonstrated to be a carcinoma on biopsy. Reproduced with permission from [44].

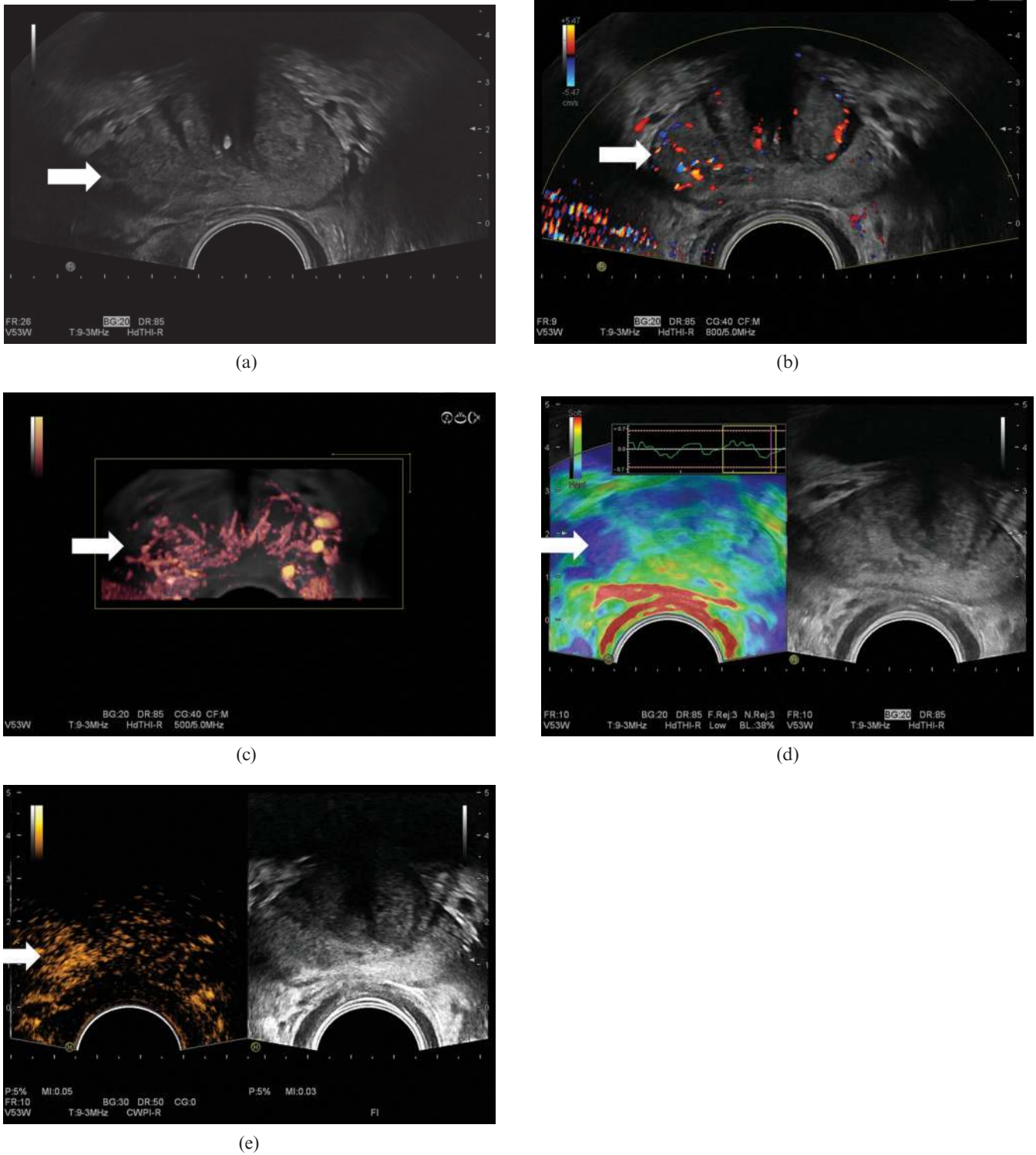


Figure 12. Prostate cancer (arrows) in a patient with a prostatic specific antigen level of 3.46 shown on greyscale (a), colour Doppler (b), three-dimensional colour Doppler (c), seen as an area of increased stiffness on elastography (d) and as a focal enhancing lesion following intravenous Sonovue® (Bracco, Milan, Italy) microbubbles using microbubble-specific imaging (e). Biopsy confirmed a Gleason 7 (3+4) prostate cancer.

improved with targeted cores *vs* sextant cores. In a study of 230 patients comparing contrast-enhanced biopsies with sextant biopsies, targeted biopsies were again found to be superior to systematic biopsy (positive biopsy rates 10.4% *vs* 5.3%, respectively) [55]. Other studies have confirmed that contrast-enhanced ultrasound improves cancer detection [56].

Aigner et al [58] compared contrast-enhanced ultrasound targeted biopsies with 10-core systematic biopsies in 44 patients. Contrast-enhanced ultrasound targeted biopsies were positive in 47% with false positives in 20% of patients, compared with positive biopsies in 9% of systematic biopsies. There was no difference in Gleason score. Mitterberger et al [59] studied 690 patients

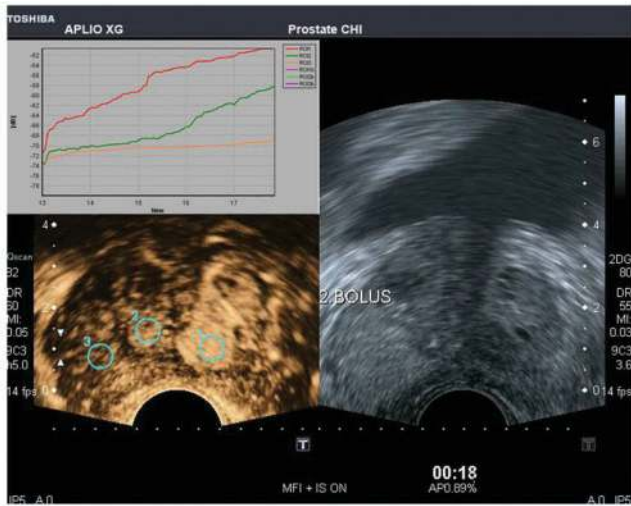


Figure 13. Transverse image of the prostate, following a bolus injection of microbubbles, with a low mechanical index mode (Micro Flow Imaging™; Toshiba, Tokyo, Japan) showing regions of interest drawn on three areas in the prostate with their time–intensity curves above. Courtesy of Professor Fisher, Necker University Hospital, Paris, France. Reproduced with permission from [56].

comparing contrast-enhanced ultrasound targeted biopsies with systematic biopsies and found significantly higher Gleason scores in the targeted group (Gleason score 6.8 *vs* 5.4). Mitterberger et al [60] in a retrospective single-centre study of 1776 patients showed that the cancer detection rate for 5 targeted cores guided by contrast-enhanced colour Doppler ultrasound was significantly better than for 10 systematic biopsy cores (10.8% *vs* 5.1%).

Sedelaar et al [61] demonstrated a correlation between increased microvessel density in foci of prostate cancer and three-dimensional contrast-enhanced power Doppler imaging. Unal et al [62] showed that contrast-enhanced

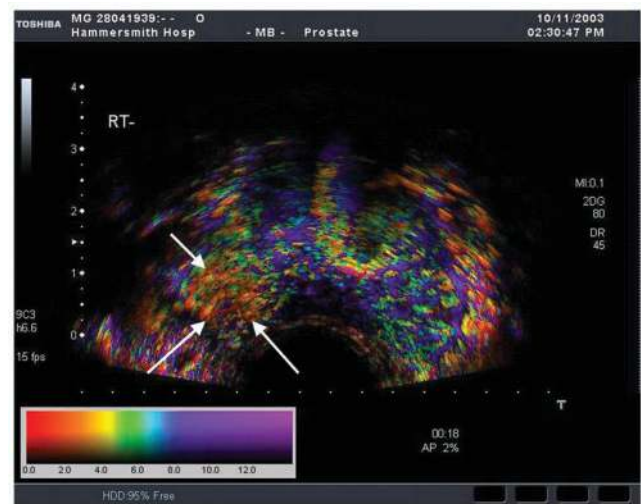
power Doppler could be used to discriminate between BPH and cancer with an accuracy of 81%.

Demonstration of blood flow changes have been used to help identify cancers. In a study using dutasteride (a dual 5 α -reductase inhibitor), which was administered prior to biopsy, a reduction in blood flow was shown in benign tissue compared with cancer [63]. Enhanced Doppler has also been used to monitor response to treatment. In a study of 68 patients followed up during treatment with enhanced power Doppler the majority showed a decrease in vascularity within a day or so following commencement of anti-androgen therapy, which paralleled falling PSA levels [64] (Figure 15). Interestingly, in two cases, there was a discrepancy in that the vascularity remained high despite a fall in PSA level. These patients had escaped from hormonal control at 6-month review. Failure to switch off neovascularity may be an early indicator of relapse, which could prompt a treatment adjustment. The emergence of angiogenesis inhibitors is also interesting and contrast-enhanced ultrasound could provide a quantitative tool to monitor these agents.

Another exciting application of microbubbles is their use as targeted agents by attaching a ligand onto their surface directed against endothelial targets, *e.g.* to highlight activated endothelium and newly formed blood vessels [65]. This technique can be used to render a tissue more conspicuous or deliver a payload of genes or drugs to a target site. Targeted microbubbles are under development that bind to specific markers or tissues, which would dramatically improve sensitivity. In a study comparing BR55 (a new antivascular endothelial growth factor receptor 2-specific bubble) and non-labelled Sonovue® (Bracco, Milan, Italy) in rat prostate cancer, both bubbles provided information in the early vascular phase, but BR55 had a late-phase binding to tumour endothelium allowing an extended window for biopsy [66]. Non-labelled Sonovue washed out and no significant accumulation of bubbles was seen in healthy prostate tissue.



(a)



(b)

Figure 14. Functional imaging of the prostate. (a) Axial B-mode ultrasound depicting a carcinoma (arrow). (b) Corresponding section of prostate with a functional overlay image (Toshiba, Tokyo, Japan) superimposed showing contrast medium bolus arrival time following an intravenous injection of microbubbles. The cancer (arrows) demonstrates an earlier arrival time than the rest of the prostate. The colour scale shows the arrival time in seconds. Reproduced with permission from [44].

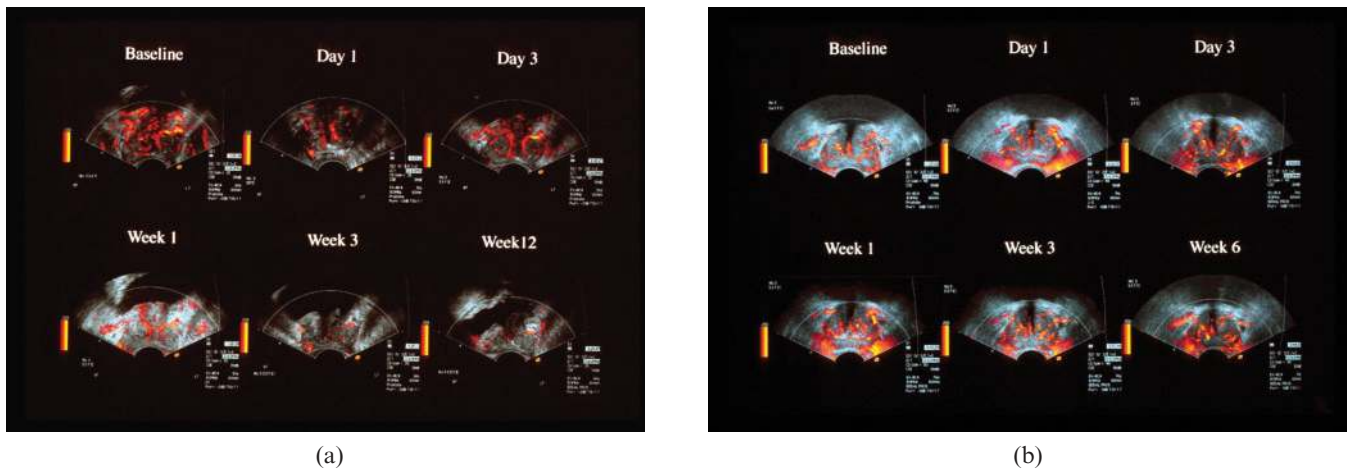


Figure 15. Two cases of carcinoma of the prostate showing differential response to anti-androgen therapy on contrast-enhanced ultrasound. (a) Sequence of contrast-enhanced power Doppler images taken from the peak in enhancement at baseline and intervals after commencement of therapy. Note the marked decrease in signals after the first week indicating good response to therapy, which was observed clinically. (b) Sequence of contrast-enhanced power Doppler images of a different patient taken from the peak in enhancement at baseline and intervals after commencement of therapy. Note in this case the signals do not decrease over the treatment period. This patient escaped from hormonal control at 6-month review. Courtesy of Dr Eckersley, Department of Imaging, Hammersmith Hospital, London, UK. Reproduced with permission from [44].

Overall contrast-enhanced ultrasound targeted biopsies improve the sensitivity of the detection of prostate cancer despite a lack of specificity, but not sufficiently to avoid systematic biopsies; therefore, the place of contrast-enhanced ultrasound is still under debate [58, 67–70].

Future promising developments include three- and four-dimensional imaging, which may depict the cancer neovascularity that is only transiently seen in the arterial phase during contrast-enhanced ultrasound.

Currently the results of large multicentre trials are awaited comparing targeted post-contrast biopsies with systematic biopsies to ascertain whether the promise of contrast-enhanced ultrasound of the prostate can be translated into clinical practice.

Elastography

This is a novel technique whereby the stiffness (Young's modulus) of a tumour can be imaged and quantified by measuring its strain under an applied stress (compression by transducer). Shear wave elastography may also be of potential value as this technique allows true quantification of Young's modulus rather than strain (a surrogate index of stiffness), as measured by current commercially available strain elastography systems [71]. In tumours, the stiffness is usually increased (Figure 12). Pallwein et al [72], in a study of 230 patients using two independent examiners, performed elastography-directed targeted biopsies followed by 10 systematic biopsies. The detection rate for elastography-targeted biopsies was significantly higher than for systematic biopsies (12.7% vs 5.6%). In another study, real-time elastography detected cancer in men with PSA values ranging from 1.25 to 4.00 ng ml⁻¹ with significantly fewer biopsy cores than systematic biopsy, with a cancer detection rate per core of 4.7-fold greater than for systematic biopsy [73].

In a study comparing elastography with T₂ weighted endorectal MRI similar sensitivity rates and negative predictive values were obtained for the detection of

prostate cancer [74]. Large trials are under way to determine whether elastography-targeted biopsies can replace systematic biopsies.

MR fusion biopsy techniques

MRI has a moderately high sensitivity and specificity for the detection and staging of prostate cancer. Recently, a new technique has emerged which allows a pre-performed MRI to be coregistered to landmarks so that real-time virtual ultrasound-guided biopsies can be performed [75–78]. Experience is limited, but this is a very promising development that would overcome the limitation of TRUS in detecting cancer while retaining the flexibility and convenience of TRUS-directed needle biopsy (Figures 16 and 17). Visualising the needle and tumour simultaneously increases the accuracy of targeted biopsy or ablative therapy.

The technique allows multiplanar biopsy planning, and Xu et al [77] showed an accuracy of 2.4 ± 1.2 mm in phantom and canine studies. Hadaschik et al [78] in a study of 106 males demonstrated that, in highly suspicious MR lesions, the *perineal* biopsy detection rate was 95.8% with a significantly higher positivity rate than non-targeted cores. They quoted that the procedural targeting error of the first 2461 biopsy cores was 1.7 mm. Further multicentre trials are necessary to evaluate this technique in cancer detection.

Conclusion

Prostate cancer is a major cause of morbidity and mortality in the UK. TRUS remains the first modality of choice to image and biopsy the prostate. However, TRUS has a poor accuracy in detection and staging of prostate cancer.

Contrast-enhanced ultrasound shows promising results allowing an assessment of tumour microvasculature, but further trials are in progress to evaluate its

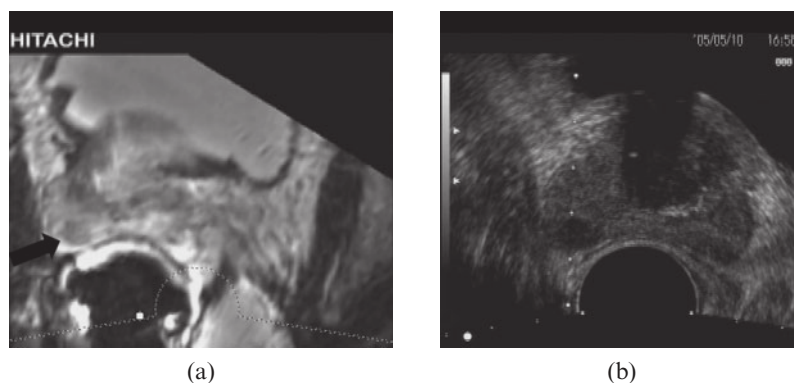


Figure 16. MR transrectal ultrasound (TRUS) fusion image showing a prostate cancer on the MR image (a; black arrow) and biopsy being performed on the TRUS (b), seen as biopsy guidance lines.

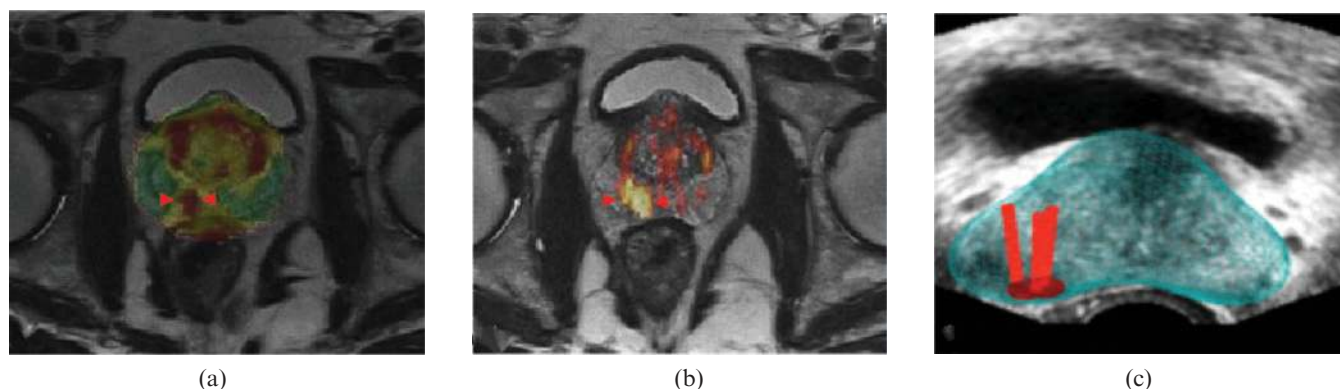


Figure 17. MR transrectal ultrasound (TRUS) fusion image. (a, b) Multiparametric axial MR images with functional information (related to diffusion-weighted MRI) identifying a cancer (arrowheads) not visible on TRUS (study not shown). (c) Fused data set, superimposing after coregistration the MR images that identify the tumour based on its reduced diffusion onto the real-time TRUS images. The red bars represent biopsy trajectories. Biopsy directed by the TRUS revealed a Gleason 7 cancer. Courtesy of Dr Erik Rud, Oslo University Hospital, Oslo, Norway.

role. Molecular techniques depicting tumour neovascularity are an exciting prospect on the horizon.

Real-time elastography has been demonstrated to improve cancer detection based on changes in tissue stiffness. In addition, a novel MR/ultrasound fusion mode is under evaluation. These new techniques may help target prostate cancer, allowing fewer biopsy cores to be performed and facilitating the detection of the important life-threatening aggressive cancers rather than indolent cancers.

References

1. Northern Ireland Cancer Registry. Cancer incidence and mortality. Belfast, UK: NICR; 2010.
2. Welsh Cancer Intelligence and Surveillance Unit. Cardiff, UK: WCISU; 2010.
3. ISD Online Information and Statistics Division, NHS Scotland. Edinburgh, UK: ISD Scotland; 2010.
4. Office for National Statistics. Registrations of cancer diagnosed in 2008, England. Series MB1 no. 39. London, UK: National Statistics; 2010.
5. Sakr WA, Grignon DJ, Haas GP, Heilbrun LK, Pontes JE, Crissman JD. Age and racial distribution of prostatic intraepithelial neoplasia. *Eur Urol* 1996;30:138–44.
6. Burford DC, Kirby M, Austoker J. Prostate Cancer Risk Management Programme information for primary care: PSA testing for asymptomatic men. Sheffield, UK: NHS Cancer Screening Programmes; 2008.
7. Prostate Cancer UK. Incidence statistics. London, UK: Prostate Cancer UK. [Cited 6 January 2008.] Available from: <http://info.cancerresearchuk.org/cancerstats/types/prostate/incidence/?a=5441#source12>
8. Jemal A, Siegel R, Ward E, Murray T, Xu J, Thun MJ. Cancer statistics, 2007. *CA Cancer J Clin* 2007;57:43–66.
9. Cooperberg MR, Broering JM, Latini DM, Litwin MS, Wallace KL, Carroll PR. Patterns of practice in the United States: insights from CaPSURE on prostate cancer management. *Curr Urol Rep* 2004;5:166–72.
10. Ilic D, O'Connor D, Green S, Wilt TJ. Screening for prostate cancer: an updated Cochrane systematic review. *BJU Int* 2011;107:882–91.
11. Djulbegovic M, Beyth R, Neuberger M, Stoffs T, Vieweg J, Djulbegovic B, et al. Screening for prostate cancer: systematic review and meta-analysis of randomised controlled trials. *BMJ* 2010;14:341.
12. Onur R, Littrup PJ, Pontes JE, Bianco FJ Jr. Contemporary impact of transrectal ultrasound lesions for prostate cancer detection. *J Urol* 2004;172:512–14.
13. Patel U, Rickards D. Handbook of transrectal ultrasound and biopsy of the prostate. London, UK: Martin Dunitz; 2002.
14. Patel U. The prostate and seminal vesicles. In: Allan P, Baxter G, Weston M, eds. *Clinical ultrasound*. 3rd edn. Edinburgh, UK: Churchill-Livingstone; 2011. pp. 572–92.
15. Kravchick S, Peled R, Ben Dor D, Dorfman D, Kesari D, Cytron S. Comparison of different local anaesthesia

- techniques during TRUS-guided biopsies: a prospective pilot study. *Urology* 2005;65:109–13.
16. Trucchi A, De Nunzio C, Mariani S, Palleschi G, Miano L, Tubaro A. Local anesthesia reduces pain associated with transrectal prostatic biopsy. A prospective randomized study. *Urol Int* 2005;74:209–13.
 17. Lee-Elliott CE, Dundas D, Patel U. Randomised trial of lidocaine vs lidocaine/bupivacaine periprostatic injection on longitudinal pain scores after prostate biopsy. *J Urol* 2004;171:247–50.
 18. Turgut AT, Dogra VS. Transrectal prostate biopsies. In: Dogra V, Saad W, eds. *Ultrasound guided procedures*. New York, NY: Thieme; 2009. pp. 85–93.
 19. Turgut AT, Olçücüoğlu E, Koşar P, Geyik PO, Koşar U. Complications and limitations related to periprostatic local anaesthesia before TRUS-guided biopsy. *J Clin Ultrasound* 2008;36:67–71.
 20. Seymour H, Perry MJ, Lee-Elliott C, Dundas D, Patel U. Pain after transrectal ultrasonography-guided prostate biopsy: the advantages of periprostatic local anaesthesia. *BJU Int* 2001;88:540–4.
 21. Obek C, Onal B, Ozkan B, Onder AU, Yalcin V, Solok V. Is periprostatic local anesthesia for transrectal ultrasound guided prostate biopsy associated with increased infectious or hemorrhagic complications? A prospective randomized trial. *J Urol* 2002;168:558–61.
 22. Webb NR, Woo HH. Antibiotic prophylaxis for prostate biopsy. *BJU Int* 2002;89:824–8.
 23. Ghani KR, Dundas D, Patel U. Bleeding after transrectal ultrasonography-guided prostate biopsy: a study of 7-day morbidity after a six-, eight- and 12-core biopsy protocol. *BJU Int* 2004;94:1014–20.
 24. Lee G, Attar K, Laniado M, Karim O. Trans-rectal ultrasound guided biopsy of the prostate: nationwide diversity in practice and training in the United Kingdom. *Int Urol Nephrol* 2007;39:185–8.
 25. Heidenreich A, Bastian PJ, Bellmunt J, Bolla M, Joniau S, Mason MD, et al. Guidelines on prostate cancer. Arnhem, the Netherlands: European Association of Urology; 2012.
 26. Sadeghi-Nejad H, Simmons M, Dakwar G, Dogra V. Controversies in transrectal ultrasonography and prostate biopsy. *Ultrasound Q* 2006;22:169–75.
 27. Loeb S, Carter HB, Berndt SI, Ricker W, Schaeffer EM. Complications after prostate biopsy: data from SEER-medicare. *J Urol* 2011;186:1830–4.
 28. Rosario DJ, Lane JA, Metcalfe C, Donovan JL, Doble A, Goodwin L, et al. Short term outcomes of prostate biopsy in men tested for cancer by prostatic specific antigen: prospective evaluation within the ProtecT study. *BMJ* 2012;344:d7894.
 29. Giannarini G, Mogorovich A, Valent F, Morelli G, De Maria M, Manassero F, et al. Continuing or discontinuing aspirin before transrectal prostate biopsy: results of a prospective randomised trial. *Urology* 2007;70:501–5.
 30. Hodge KK, McNeal JE, Terris MK, Stamey TA. Random systematic versus directed ultrasound guided transrectal core biopsies of the prostate. *J Urol* 1989;142:71–4.
 31. NHS Cancer Screening Programmes. Undertaking a transrectal ultrasound guided biopsy of the prostate. PRCMP Guide no. 1. Sheffield, UK: NHS Cancer Screening Programmes; 2006.
 32. Djavan B, Margreiter M. Biopsy standards for detection of prostate cancer. *World J Urol* 2007;25:11–17.
 33. Eichler K, Hempel S, Wilby J, Myers L, Bachmann LM, Kleijnen J. Diagnostic value of systematic biopsy methods in the investigation of prostate cancer: a systematic review. *J Urol* 2006;175:1605–12.
 34. Loch T. Urologic imaging for localised prostate cancer in 2007. *World J Urol* 2007;25:121–9.
 35. Gosselaar C, Roobol M, Roemeling S, Wolters T, van Leenders G, Schroder F. The value of an additional hypochoic lesion-directed biopsy core for detecting prostate cancer. *BJU Int* 2008;101:685–90.
 36. Toi A, Neill M, Lockwood G, Sweet J, Tammsalu L, Fleshner N. The continuing importance of transrectal ultrasound identification of prostatic lesions. *J Urol* 2007;177:516–20.
 37. Raja J, Ramachandran N, Munneke G, Patel U. Current status of transrectal ultrasound-guided prostate biopsy in the diagnosis of prostate cancer. *Clin Radiol* 2006;61:142–53.
 38. Purohit R, Shinohara K, Meng M, Carroll PR. Imaging clinically localized prostate cancer. *Urol Clin North Am* 2003;30:279–93.
 39. Turgut A, Dogra V. Prostatic cancer: evaluation using transrectal sonography. In: Hayat M, ed. *Methods of cancer diagnosis, therapy and prognosis*. New York, NY: Elsevier; 2008. pp. 499–520.
 40. Halpern E, Strup S. Using gray scale and color and power Doppler sonography to detect prostatic cancer. *AJR Am J Roentgenol* 2000;174:623–7.
 41. Turgut A, Olcucuoglu E, Kosar P, Geyik PO, Koşar U, Dogra V. Power Doppler ultrasonography of the feeding arteries of the prostate gland: a novel approach to the diagnosis of prostate cancer? *J Ultrasound Med* 2007;26:875–83.
 42. Pallwein L, Mitterberger M, Pelzer A, Bartsch G, Strasser H, Pinggera GM, et al. Ultrasound of the prostate cancer: recent advances. *Eur Radiol* 2008;18:707–15.
 43. Bigler SA, Deering RE, Brawer MK. Comparison of microscopic vascularity in benign and malignant prostate tissue. *Hum Pathol* 1993;24:220–6.
 44. Padhani AR, Harvey CJ, Cosgrove DO. Angiogenesis imaging in the management of prostate cancer. *Nat Clin Pract Urol* 2005;12:596–607.
 45. Wijkstra H, Wink M, de la Rosette J. Contrast specific imaging in the detection and localisation of prostate cancer. *World J Urol* 2004;22:346–50.
 46. Leen E, Averkiou M, Arditi M, Burns P, Bokor D, Gauthier T, et al. Dynamic contrast enhanced ultrasound assessment of the vascular effects of novel therapeutics in early stage trials. *Eur Radiol* 2012;22:1442–50.
 47. Harvey CJ, Pilcher J, Eckersley R, Blomley MJK, Cosgrove DO. Advances in ultrasound. *Clin Radiol* 2002;57:157–77.
 48. Cosgrove DO, Eckersley RJ, Blomley M, Harvey CJ. Quantification of blood flow. *Eur Radiol* 2001;11:1338–44.
 49. Eckersley RJ, Cosgrove DO, Blomley MJ, Hashimoto H. Functional imaging of tissue response to bolus injection of ultrasound contrast agent. Proceedings of the 1998 IEEE Ultrasonics Symposium; 5–8 October 1998; Sendai, Japan. New York, NY: IEEE.
 50. Goossen TE, de la Rosette JJ, Hulsbergen-van de Kaa CA, van Leenders GJ, Wijkstra H. The value of dynamic contrast enhanced power Doppler ultrasound imaging in the localization of prostate cancer. *Eur Urol* 2003;43:124–31.
 51. Wei K, Jayaweera AR, Firoozan S, Linka A, Skyba DM, Kaul S. Quantification of myocardial blood flow with ultrasound induced destruction of microbubbles administered as a constant venous infusion. *Circulation* 1998;97:473–83.
 52. Halpern EJ, Rosenberg M, Gomella LG. Prostate cancer: contrast enhanced US for detection. *Radiology* 2001;219:219–25.
 53. Frauscher F, Klauser A, Halpern EJ. Advances in ultrasound for the detection of prostate cancer. *Ultrasound Q* 2002;18:135–42.
 54. Frauscher F, Klauser A, Halpern EJ. Detection of prostate cancer with a microbubble contrast agent. *Lancet* 2001;357:1849–50.
 55. Frauscher F, Klauser A, Volgger H, Halpern EJ, Pallwein L, Steiner H, et al. Comparison of contrast-enhanced color Doppler targeted biopsy with conventional systematic biopsy: impact on prostate cancer. *J Urol* 2002;167:1648–52.

56. Harvey CJ, Sidhu P. Ultrasound contrast agents in genitourinary imaging. *Ultrasound Clin* 2010;5:489–506.
57. Halpern EJ, Frauscher F, Rosenberg M, Gomella LG. Directed biopsy during contrast enhanced sonography of the prostate. *AJR Am J Roentgenol* 2002;178:915–19.
58. Aigner F, Pallwein L, Mitterberger M, Pinggera GM, Mikuz G, Horninger W, et al. Contrast-enhanced ultrasonography using cadence-contrast pulse sequencing technology for targeted biopsy of the prostate. *BJU Int* 2009;103:458–63.
59. Mitterberger M, Pinggera GM, Horninger W, Bartsch G, Strasser H, Schäfer G, et al. Comparison of contrast enhanced color Doppler targeted biopsy to conventional systematic biopsy: impact on Gleason score. *J Urol* 2007;178:464–8.
60. Mitterberger M, Aigner F, Horninger W, Ulmer H, Cavuto S, Halpern EJ, et al. Comparative efficiency of contrast-enhanced colour Doppler ultrasound targeted versus systematic biopsy for prostate cancer detection. *Eur Radiol* 2010;20:2791–6.
61. Sedelaar JP, Van Leenders GJ, Hulsbergen-Van De Kaa CA, van der Poel HG, van der Laak JA, Debruyne FM, et al. Microvessel density: correlation between contrast ultrasonography and histology of prostate cancer. *Eur Urol* 2001;40:285–93.
62. Unal D, Sedelaar JP, Aarnink RG, van Leenders GJ, Wijkstra H, Debruyne FM, et al. Three-dimensional contrast-enhanced power Doppler ultrasonography and conventional examination methods: the value of diagnostic predictors of prostate cancer. *BJU Int* 2000;86:58–64.
63. Mitterberger M, Pinggera G, Horninger W, Strasser H, Halpern E, Pallwein L, et al. Dutasteride prior to contrast-enhanced colour Doppler ultrasound prostate biopsy increases prostate cancer detection. *Eur Urol* 2008;53:112–17.
64. Eckersley RJ, Butler-Barnes J, Blomley MJ, Cosgrove DO. Quantification microbubble enhanced transrectal ultrasound (TRUS) as a tool for monitoring anti-androgen therapy in prostate carcinoma. *Radiology* 1998;209:310.
65. Smeenge M, Mischi M, Laguna Pes M, de la Rosette J, Wijkstra H. Novel contrast-enhanced ultrasound imaging in prostate cancer. *World J Urol* 2011;29:581–7.
66. Tardy I, Pochon S, Theraulaz M, Emmel P, Passantino L, Tranquart F, et al. Ultrasound molecular imaging of VEGFR2 in a rat prostate tumor model using BR55. *Invest Radiol* 2010;45:573–8.
67. Wink M, Frauscher F, Cosgrove D, Chapelon JY, Palwein L, Mitterberger M, et al. Contrast-enhanced ultrasound and prostate cancer: a multicentre European research coordination project. *Eur Urol* 2008;54:982–92.
68. Piscaglia F, Nolsøe C, Dietrich CF, Cosgrove DO, Gilja OH, Bachmann Nielsen M, et al. The EFSUMB guidelines and recommendations on clinical practice of contrast enhanced ultrasound (CEUS): update 2011. *Ultraschall Med* 2012;33:33–59.
69. Sano F, Terao H, Kawahara T, Miyoshi Y, Sasaki T, Noguchi K, et al. Contrast-enhanced ultrasonography of the prostate: various imaging findings that indicate prostate cancer. *BJU Int* 2010;107:1404–10.
70. Strazdina A, Krumina G, Sperga M. The value and limitations of contrast-enhanced ultrasound in the detection of prostate cancer. *Anticancer Res* 2011;31:1421–6.
71. Hoskins P. Principles of ultrasound elastography. *Ultrasound* 2012;20:8–15.
72. Pallwein L, Mitterberger M, Struve P, Horninger W, Aigner F, Bartsch B, et al. Comparison of sonoelastography guided biopsy with systematic biopsy: impact on prostate cancer detection. *Eur Radiol* 2007;17:2278–85.
73. Aigner F, Pallwein L, Junker D, Schafer G, Mikuz G, Pedross F, et al. Value of real-time elastography targeted biopsy for prostate cancer detection in men with prostatic specific antigen 1.25 or greater and 4 ng/ml or less. *J Urol* 2010;184:913–17.
74. Aigner F, Pallwein L, Schocke M, Lebovici A, Junker D, Schafer G, et al. Comparison of real-time sonoelastography with T₂-weighted endorectal magnetic resonance imaging for prostate cancer detection. *J Ultrasound Med* 2011;30:643–9.
75. Ukimura O, Gill IS. Image-fusion, augmented reality, and predictive surgical navigation. *Urol Clin North Am* 2009;36:115–23.
76. Pinto PA, Chung PH, Rastinehad AR, Baccala AA Jr, Kruecker J, Benjamin CJ, et al. Magnetic resonance imaging/ultrasound fusion guided prostate biopsy improves cancer detection following transrectal ultrasound biopsy and correlates with multiparametric magnetic resonance imaging. *J Urol* 2011;186:1281–5.
77. Xu S, Kruecker J, Turkbey B, Glossop N, Singh AK, Choyke P, et al. Real-time MRI-TRUS fusion for guidance of targeted prostate biopsies. *Comput Aided Surg* 2008;13:255.
78. Hadaschik B, Kuru T, Tulea C, Rieker P, Popeneciu IV, Simpfendorfer T, et al. A novel stereotactic prostate biopsy system integrating pre-interventional magnetic resonance imaging and live ultrasound fusion. *J Urol* 2011;186:2214–20.